Chlorine-induced de-reconstruction on Au(001) and Cl-adsorbed layers

1995 J. Phys.: Condens. Matter 7 5163

(http://iopscience.iop.org/0953-8984/7/27/005)

J. Phys.: Condens. Matter 7 (1995) 5163–5176. Printed in the UK

Chlorine-induced de-reconstruction on Au(001) and Cl-adsorbed layers

H Iwai, M Okada†, K Fukutani and Y Murata

Institute for Solid State Physics, The University of Tokyo, 7-22-1 Roppongi, Minato-ku, Tokyo 106, Japan

Received 20 September 1994, in final form 20 February 1995

Abstract. Chlorine adsorption on the reconstructed Au(001) surface causes de-reconstruction to a 1×1 structure at room temperature above an absolute coverage of ~0.06. The de-reconstruction is considered to be due to the chemical-bonding effect between the adsorbate and the substrate in the same way as that in potassium adsorption on Au(001). Various superlattice patterns in low-energy electron diffraction are observed at low temperature (~100 K) which form a one-dimensional structure depending on coverage. The coverage dependence of the thermal desorption spectra for the Cl and Cl_2 species suggests a frustrated desorption from one-dimensional chains formed by adsorbates.

1. Introduction

It is well known that the clean Au(001) surface is reconstructed into a superstructure, referred to as 5×20 [1]. The atomic structure of this surface has been extensively examined by various experimental methods including low-energy electron diffraction (LEED) [2], transmission electron microscopy [3], and scanning tunnelling microscopy (STM) [4, 5]. By these methods, the top-layer of the Au(001) clean surface has been concluded to be reconstructed to a hexagonal structure similar to an fcc(111) surface.

On the other hand, after oxygen ion bombardment a metastable phase of the 1×1 structure has been observed which undergoes an irreversible phase transition to the 5×20 structure at 373 K [6]. This means that the 1×1 structure exists as a metastable state, and that by excitation it is possible to transform the 5×20 phase to the 1×1 phase.

It is worth noting the reconstruction of the Au(110) and Au(111) surfaces. The Au(110) surface is reconstructed to a 2×1 surface structure of missing-row type, on which the highest density of {111} surface facets appears. Although the hexagonal (111) surface was expected to be ultimately stable and to show no structural change, it was found that the Au(111) surface is indeed reconstructed into a compressed structure with higher atomic density [7]. Thus, all Au surfaces, including high-index planes [8], are of reconstructed hexagonal structure.

On the other hand, alkali-metal adsorption sometimes causes adsorption-induced reconstruction by transferring electrons from the adsorbate to the surface producing a surface with higher atomic density. Pioneering work on the adsorption of alkali metals on Ni(110) was carried out by Gerlach and Rhodin [15]. In the case of Au(110), the clean surface forms a 2×1 missing row structure with {111} facets as mentioned above. By cesium

† Present address: Oak Ridge National Laboratory, PO Box 2008, Oak Ridge, TN 37831-6057, USA.

0953-8984/95/275163+14$19.50

adsorption on Au(110), a 3×1 phase stabilizes at an absolute coverage θ_a of 0.05 [16]. On this 3×1 surface, two of three adjacent $[1\bar{1}0]$ top-layer rows are missing producing larger {111} facets [17]. Thus, the reconstruction on Au(001) and Au(110) clean surfaces is closely related with the reconstruction induced by alkali-metal adsorption.

Previously, we studied systems of potassium adsorption on Ag(001) and Au(001) surfaces at room (RT) and low temperatures (LT) by LEED and measured the workfunction change ($\Delta\phi$) [18, 19]. On Au(001), we found that de-reconstruction, transformation from the reconstructed structure (5×20) to the unreconstructed structure (1×1), is caused by potassium adsorption. This de-reconstruction to the 1×1 structure appears at $\theta_a = 0.08$ [19]. It is considered to be due to the chemical interaction of a K atom with the substrate followed by the vanishing of a soliton. However, the origin of the de-reconstruction is not well understood. Reconstruction to the 2×1 structure (missing-row) was found on both Ag(001) and Au(001), on which {111} facets are formed. The potassium-induced reconstruction on Ag (001) has been explained by a calculation performed by Christensen and Jacobsen, but reconstruction on Au(001) was not expected in their theoretical result [20].

We expect that the origin of these reconstructions is the same for Au(001), Au(110) and alkali-induced structures. Theoretically, it is pointed out that the increase of the surface electron density for the delocalized s, p-state introduces an increase in the cohesive energy [9]. According to a recent study of the potential-induced reconstruction by STM, reconstructed 'hex'-domains grow along the direction of the rows, Au atoms being supplied from islands [4, 5]. However, the driving force for the reconstruction has not clearly been understood, in spite of several efforts from experimental [6, 10, 11] and theoretical [12–14] standpoints. In contrast to alkali metals, a halogen atom is a strong electron acceptor (large electron affinity). If the charge density in a metal surface is important for reconstruction, halogen atom adsorption should provide us with a key to understanding the reconstruction mechanism. The atomic number of chlorine is close to that of potassium. In previous studies, de-reconstruction was observed in bromine and iodine adsorption on Au(001) [21, 22]. In the present paper, we report the de-reconstruction process induced by chlorine adsorption on Au(001). Comparing with that in potassium on Au(001), we discuss the origin of de-reconstruction. We also report superlattice patterns observed in LEED at low temperature ($\sim$100 K) at various Cl coverages. We propose a series of one-dimensional chains as a model which explains these LEED patterns and the thermal-desorption spectrum (TDS).

2. Experiment

Experiments were performed in an ultra-high vacuum (UHV) chamber, the base pressure of which was 8×10^{-11} Torr, equipped with Varian fourfold grid LEED optics. In this system we observed LEED and measured $\Delta\phi$ by the retarding field method. A TDS was taken using a quadrupole mass spectrometer covered by a stainless-steel cup with an aperture. The heating rate was about 1 K s^{-1} and the desorbed species were detected in the surface normal direction. The sample temperature was measured by a thermocouple of Pt–PtRh 13%. The intensity of the LEED spots was measured with high sensitivity by a video camera using a silicon intensifier target tube.

The Au(001) specimen was cut from a single crystal Au rod and was mechanically polished. The surface was cleaned by repeated cycles of Ar^+ ion bombardment (500 eV, 4 μA, 10 min) and annealing (700 K, 10 min) in the UHV chamber until 5×20 sharp spots were observed by LEED and no impurity signals were detected by Auger electron spectroscopy (AES). The chlorine beam was generated from an electrolytic cell containing

solid AgCl [23]; cathode and anode were made of a Pt mesh and a spiral Ag wire, respectively. The typical dose time was 10 min for saturation. Analysing the beam revealed a large component of a mass 35 signal (^{35}Cl) and small components of mass 18 and 70 signals (H_2O and $^{35}Cl_2$, respectively). The water yield was less than one tenth of the Cl yield without calibration of the mass spectrometer's sensitivity.

The relative coverage of Cl on the surface was estimated from the integrated TDS intensity, because an AES spectrum is rapidly modified by electron-stimulated desorption of Cl. Furthermore, the absolute coverage at saturation is estimated to be unity from a series of superstructures, assuming that adsorbed Cl atoms form these structures, as discussed later.

3. Results

3.1. TDS of Cl and Cl_2 from Au(001)

Figure 1 shows the coverage dependence of the Cl (figure 1(*a*)) and Cl_2 (figure 1(*b*)) TDS signals for adsorption at RT. The relative coverage θ_r shown is tentatively defined as the ratio of the integrated intensity of each Cl spectrum in figure 1(*a*) to that of the Cl spectrum at saturation coverage. The spectrum for the highest coverage in figure 1(*a*) corresponds to the saturation coverage of Cl on Au(001) at RT, no change being observed in TDS after further exposure. The thermal-desorption spectrum for the specimen adsorbed at LT is essentially the same as that shown in figure 1, except for a small desorption peak which corresponds to species physisorbed at ~150 K with $\theta_r > 1$.

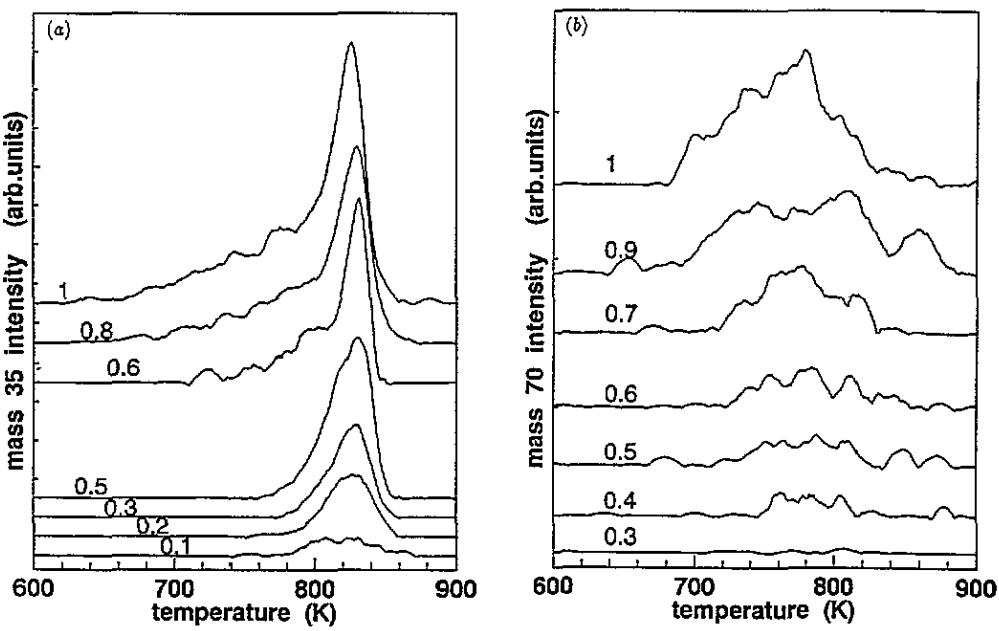

Figure 1. TDS from Cl on Au(001) at RT for (*a*) mass 35 (^{35}Cl) and (*b*) mass 70 ($^{70}Cl_2$). The relative coverage θ_r is listed in each spectrum.

A prominent sharp peak at 820 K develops with increasing coverage in the Cl spectrum shown in figure 1(*a*). Its position hardly changes with coverage. A broad peak in the lower-temperature range clearly appears at a coverage (θ_r) larger than 0.5. In the Cl_2 spectrum, a broad peak was observed between 650 K and 800 K for $\theta_r > 0.4$. It shows a similar behaviour to that of the broad peak in the Cl spectrum. The onset temperature of both of the peaks decreases with increasing coverage. Both appear at almost the same temperature for each coverage. Figure 2 shows the desorption energy of the broad peak in the Cl spectrum and the peak in the Cl_2 spectrum, which is estimated from a fit to the Redhead equation for second-order desorption [24]

$$\frac{N_p}{N} = \frac{1}{4}\left\{\exp\left[-\frac{E_d}{2R}\left(\frac{1}{T_p} - \frac{1}{T}\right)\right] + \left(\frac{T}{T_p}\right)^2 \exp\left[-\frac{E_d}{2R}\left(\frac{1}{T} - \frac{1}{T_p}\right)\right]\right\}^2 \quad (1)$$

where N, T, E_d and R are the desorption rate, temperature, desorption energy and gas constant, respectively. N_p is the desorption rate at the temperature T_p at which the peak appears in TDS. The desorption energy of both peaks is about 2 eV irrespective of the coverage, as can be seen in figure 2. Therefore, we regard the broad peak in the Cl spectrum as being produced by cracking of desorbed Cl_2 molecules in the mass spectrometer. The dominant peak of the Cl spectrum is broader at low coverages than at high coverages. This may suggest that the broad peak is confined in the dominant peak at low coverage. In TDS of Br on Au(001), I on Au(001) and Cl on Au(111) [21, 22, 25, 26], two peaks similar to those in the spectrum shown in figure 1(*a*) have been observed, and it was suggested that the lower-temperature peak is produced by cracking a fraction of the diatomic species.

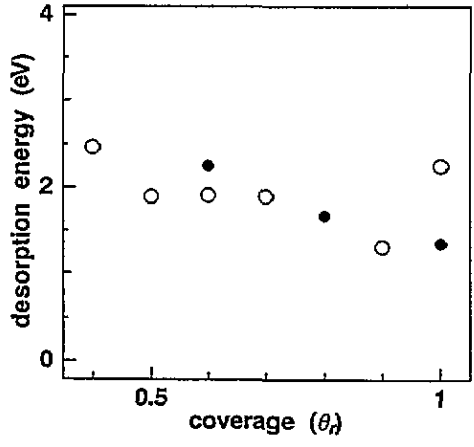

Figure 2. Desorption energy as a function of coverage estimated from broad peaks of the Cl (full circles) and Cl_2 (open circles) spectra.

Figure 3 shows the integrated intensity in the Cl_2 spectrum as a function of the relative coverage, demonstrating a linear relation. The coverage θ_r itself indicates the integrated intensity of the Cl TDS at the same dose time. By the linear relation in figure 2 it is shown that θ_r is proportional to the true relative coverage [27]. Absolute coverage will be estimated from this result in a later section.

3.2. *De-reconstruction on Au(001)*

Figure 4 shows the change of LEED patterns when Cl is adsorbed on Au(001) at RT. All LEED patterns have equivalent double domains. Figure 4(*a*) is the LEED pattern for the

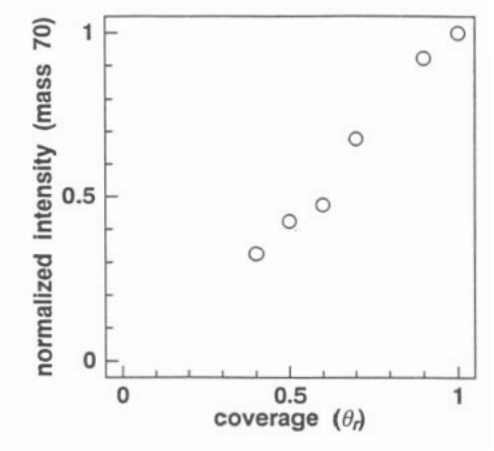

Figure 3. Integrated peak intensity of the Cl_2 TDS from Cl on Au(001) as a function of the relative coverage, which is obtained from the integrated TDS intensity for mass 35.

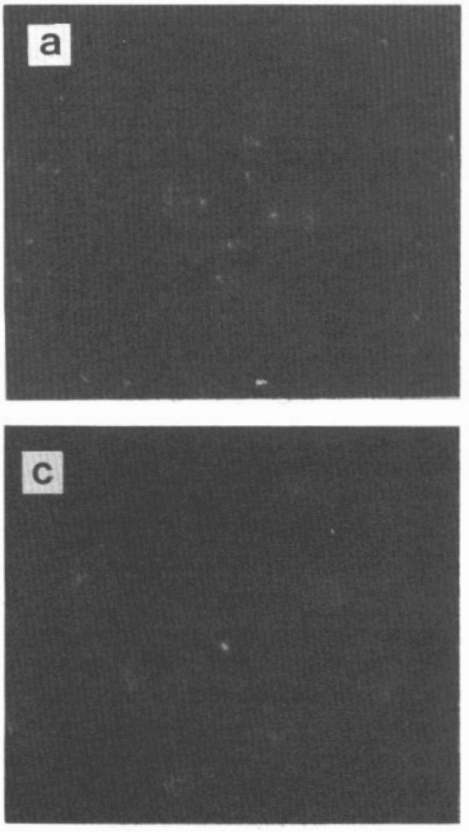

Figure 4. LEED patterns of Cl on Au(001) at RT. (*a*) Clean Au(001) pattern, E_p = 48 eV. (*b*) 1 × 1 ($\theta_r \geqslant 0.4$), E_p = 60 eV. (*c*) c(2 × 2) ($\theta_r \sim 1$), E_p = 60 eV.

clean 5 × 20 surface. The 5 × 20 pattern changes gradually into the 1 × 1 pattern (figure 4(*b*)). As the coverage increases, streaks in the ⟨11⟩ direction passing through the (1/2 1/2) and other equivalent spots appear at $\theta_r \geqslant 0.5$. Finally, the pattern turns into the c(2 × 2) type at $\theta_r \sim 1$ (figure 4(*c*)). These half order spots are slightly diffuse, as can be seen in figure 4(*c*). We consider this to be caused by thermal fluctuation of adsorbed Cl. Figure 5 shows the

LEED intensity change of the (10) (full curve), (1/2 1/2) (broken curve), and (1/5 0) (dotted curve) spots as a function of Cl coverage on the Au(001)–5 × 20 surface. The intensity of the (10) spot increases with increasing coverage, while the (1/5 0) spot intensity decreases. Therefore, we consider that Cl adsorption causes the de-reconstruction of Au(001) from 5 × 20 to 1 × 1. Another prominent feature is that the intensities of the (10) and (1/5 0) spots remain constant until $\theta_r \sim 0.06$. This indicates that the de-reconstruction from the 5 × 20 to 1 × 1 structure on the substrate occurs from $\theta_r \sim 0.06$. It is to be noted that similar intensity variation of LEED spots is observed at other primary electron energies from 15–200 eV.

3.3. LEED patterns at low temperature

When the sample was cooled down to 100 K after Cl adsorption at RT, various superlattice patterns were observed at $\theta_r \geqslant 0.40$, as shown in the left-hand parts of figure 6(*a*)–(*e*). As stated above, the substrate has already changed to the 1 × 1 structure at these coverages before cooling. Characteristic features of these patterns are as follows.

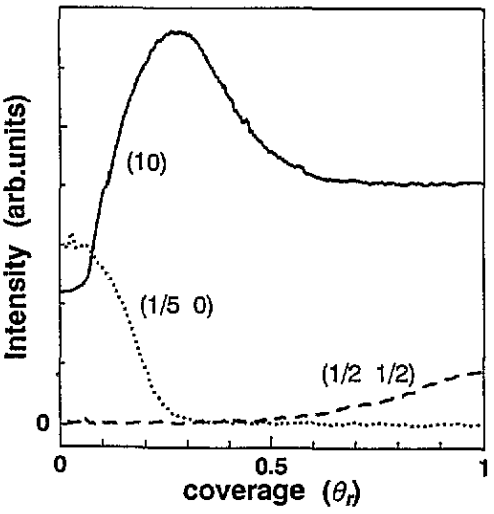

Figure 5. Intensity change of the LEED spots for (10) (full curve), (1/2 1/2) (broken curve), and (1/5 0) (dotted curve) as a function of Cl coverage in the sequence of Cl adsorption on the Au(001)-5 × 20 surface at RT. $E_p = 60$ eV.

(1) They appear suddenly below ~150 K. The spots in all patterns are aligned in the ⟨11⟩ direction parallel to the streak observed at RT. The length of the unit cell for these superlattices contracts until $\theta_r = 0.5$ and expands at $\theta_r > 0.5$ with increasing coverage.

(2) Every other superlattice spot is missing on the row along the ⟨11⟩ direction through the (00) spot, for example all (n/10 n/10) spots in the LEED pattern shown in figure 6(*a*), where n is an odd number. These spots are missing for a primary electron energy from 15–200 eV. On the other hand, most of the superlattice spots are observed on the row along the ⟨11⟩ direction through the {10} spot, for example all (n/10 1–n/10) spots in figure 6(*a*), where n is an integral number.

(3) At $\theta_r > 0.5$ (figure 6(*c*)–(e)), the intensity of the superlattice spots around integral- and half-order spots of c(2 × 2) are enhanced suggesting that these structures consist of c(2 × 2) terraces.

(4) These superlattice patterns change to c(2 × 2) after further deposition of Cl at LT (not shown in the figure).

(5) When the sample temperature is elevated beyond ~800 K and some Cl atoms are thermally desorbed, at LT a different LEED pattern is observed (figure 7). The coverage of this pattern estimated from the TDS integrated intensity is 0.34, at which the sharp 1×1 pattern cannot be obtained by adsorption at RT.

When chlorine is adsorbed at LT, no superlattice structures appear on the surface. At $\theta_r > 0.4$, streaks are observed in the ⟨01⟩ direction passing through (1/2 1/2), with a weak 5×20 pattern, as shown in figure 8. This result shows that the superlattice structures seen in figures 6 and 7 are formed only on the de-reconstructed surface that is achieved by Cl adsorption at RT. The streak direction of the pattern for adsorption at LT is 45° off that observed for adsorption at RT. When we observe on the single-domain 5×20 surface, this streak runs along a row of the $n/5$ order spots on the clean surface. At higher coverages, only the integral spots remain with high background.

When the sample temperature is elevated from LT at $\theta_r \sim 0.5$, the LEED pattern changes from 5×20 to 1×1 at 200 ~ 300 K indicating de-reconstruction of the surface. The sharp 1×1 pattern remains until about 800 K, at which the main peak in TDS grows (see figure 1(*a*)). After annealing above 820 K the 5×20 pattern appears as a result of Cl desorption. This indicates that the de-reconstructed 1×1 structure is not a metastable phase but stabilized by chlorine atoms, because the clean metastable Au(001)-1×1 surface is reconstructed to the 5×20 surface at 373 K [6].

4. Discussion

4.1. Structure model for superlattice patterns

In this section, we discuss the structure model of the superlattice patterns shown in figures 6 and 7. The unit cells can be written as $(m\sqrt{2} \times \sqrt{2})$R45°: $(6\sqrt{2} \times \sqrt{2})$R45° at $\theta_r \sim 0.34$ (figure 7), $(5\sqrt{2} \times \sqrt{2})$R45° at $\theta_r \sim 0.40$ (figure 6(*a*)), $(4\sqrt{2} \times \sqrt{2})$R45° at $\theta_r \sim 0.50$ (figure 6(*b*)), $(6\sqrt{2} \times \sqrt{2})$R45° at $\theta_r \sim 0.66$ (figure 6(*c*)), $(8\sqrt{2} \times \sqrt{2})$R45° at $\theta_r \sim 0.80$ (figure 6(*d*)), $(10\sqrt{2} \times \sqrt{2})$R45° at $0.8 < \theta_r < 1$ (figure 6(*e*)) and c(2 × 2) at $\theta_r \sim 1$. These relative coverages except for the case of $\theta_r \sim 0.34$ were determined from the Cl dose time calibrated by the TDS integrated intensity. We consider that a one-dimensional structure is formed along the ⟨11⟩ direction and the length of the unit cell contracts until $\theta_r \sim 0.5$ and expands above $\theta_r \sim 0.5$ with increasing coverage.

Since the spots of superlattices in figure 6 are intense, the substrate atom might be displaced from the 1×1 lattice point. As discussed in below, however, the phase transition temperature of these superlattices to 1×1 (~150 K) is lower than that of the de-reconstruction (~200 K), and seems to be too low for Au displaced structures. Therefore, in the present paper we assume that superlattices are formed by adsorbed Cl; the possibility of substrate displacement will be discussed later.

From both the symmetry and the extinction relation of spots in these LEED patterns, structure models are inferred, as shown in the right-hand side of figures 6 and 7. As an example, we describe the structure of figure 6(*a*), $(5\sqrt{2} \times \sqrt{2})$R45°, in the kinematical picture. The Cl and Au atoms are denoted by shaded and open circles, respectively, in the right-hand side of the figure. The unit cell is enclosed by a full curve, with x' and y' axes also shown in the figure. This coordinate system is taken for simplicity as rotated by 45° from the x and y coordinate system in the Bravais lattice. The geometry of the four Cl atoms in the unit cell is given by (0 0), (1/2–*a* 1/2–*b*), (1/2+*a* 5/2) and (0 3–*b*), where the site of Cl atoms is given with respect to a Au lattice point, i.e. a and b are the displacement of the Cl position from the Au lattice point. In order to reproduce the

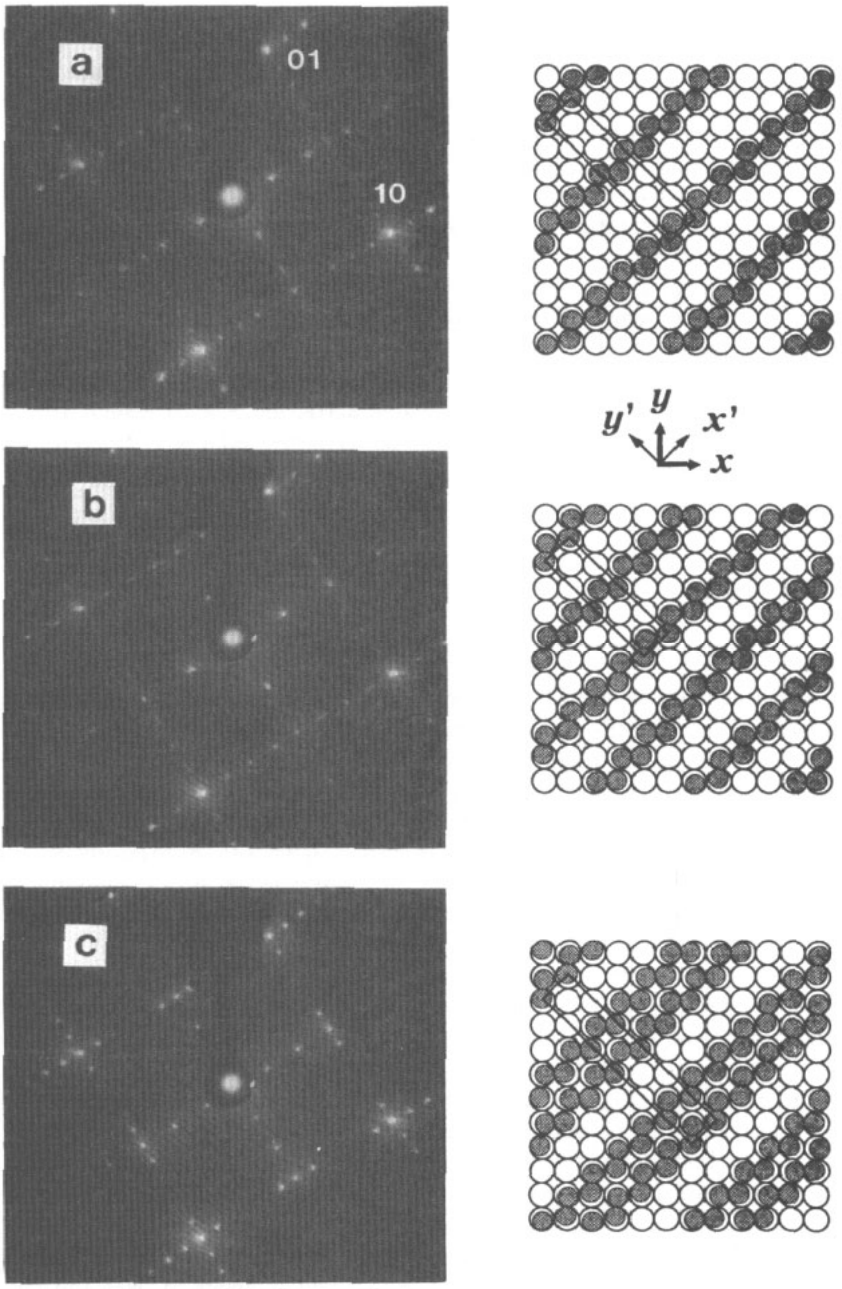

Figure 6. LEED patterns of Cl on Au(001) at LT, when Cl is adsorbed at RT. These patterns appear suddenly at ~150 K; (*a*) $(5\sqrt{2}\times\sqrt{2})$R45° ($\theta_r \sim 0.40$), (*b*) $(4\sqrt{2}\times\sqrt{2})$R45° ($\theta_r \sim 0.50$), (*c*) $(6\sqrt{2}\times\sqrt{2})$R45° ($\theta_r \sim 0.66$), (*d*) $(8\sqrt{2}\times\sqrt{2})$R45° ($\theta_r \sim 0.80$) and (*e*) $(10\sqrt{2}\times\sqrt{2})$R45° ($0.80 < \theta_r < 1$). $E_p = 60$ eV. The right-hand side shows structure models corresponding to each LEED pattern. Adsorbed Cl atoms are shown by shaded circles and substrate Au atoms are shown by open circles. The relative coverage is determined from the Cl dose time.

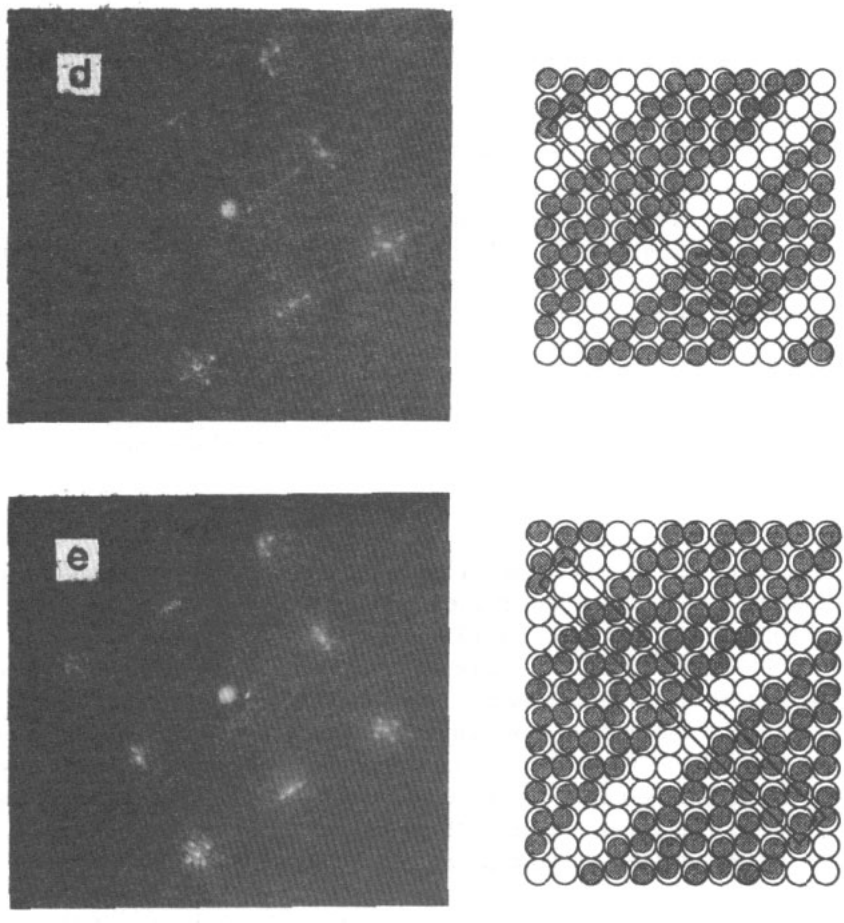

Figure 6. (Continued)

extinction relation of the LEED spots, the Cl atoms have to be displaced from the substrate lattice. The diffraction intensity of $(n'/5\ 0)$ spots vanishes for odd n', while the intensity of $(n'/5\ 1)$ reflections is finite, where the number n' representing the index of the spot is different from n in the Bravais lattice. The $(n'/5\ 0)$ and $(n'/5\ 1)$ spots are given by the $(n/10\ n/10)$ and $(n/10\ 1-n/10)$ spots, respectively, in the x and y coordinate system. In the case of $(4\sqrt{2} \times \sqrt{2})$R45°, the geometry of the four Cl atoms is given by (0 0), (1/2–a 1/2–b), (1/2+a 2) and (0 5/2–b), as indicated in the right-hand side of figure 6(b). This geometry also reproduces the LEED pattern.

Although the adsorption site of Cl atoms is not determined, the most probable adsorption site is considered to be the site with the highest coordination number, i.e. the slightly displaced fourfold hollow site, because the chemical-bonding effect is important for the de-reconstruction of the substrate surface, similar to K on Au(001) [19], as described below. However, the models in figures 6 and 7 are drawn by near on-top site just for convenience as it is easy to understand that adsorbed Cl is slightly displaced from the substrate lattice point.

In the present case, the superlattice modulated by c(2 × 2) was observed at $\theta_r \geqslant 2/3$ (figure 6(c)–(e)). This result definitely indicates the existence of a c(2×2) short-range order.

In the models at $\theta_r \geqslant 2/3$, the terrace of the adsorbed Cl layer is shown as locally forming a c(2 × 2) structure, which is consistent with the LEED results. The terrace width increases with increasing coverage, finally leading to the c(2 × 2) structure at the saturation coverage. The LEED pattern in figure 4(*b*) has streaks in a direction connecting superlattice spots which are observed at LT below saturation coverage. This implies that one-dimensional chains of adsorbed Cl atoms are distributed with random interchain distance at RT.

In a one-dimensional chain, pairs of Cl atoms seem to form dimers similar to Cl_2 molecules. The Cl–Cl bonding interaction in Cl adsorption on metal surfaces has been theoretically demonstrated by Ishida [28]. Furthermore, the arrangement of the Cl dimers on Au(001) at LT is similar to the molecular ordering in solid chlorine [29]. It is worth noting that the freezing point of solid chlorine is 113 K, close to the temperature at which these superlattice patterns appear, ~150 K. At $\theta_r = 1$, the radius of an adsorbed chlorine atom, r_{Cl}, should be smaller than that of an Au atom, r_{Au}, i.e. $r_{Cl} < r_{Au} = 1.44$ Å. This relation is satisfied for the covalent-bond radius of the Cl atom, $r_{Cl} = 0.99$ Å, whereas the Cl^- radius of 1.81 Å is longer than r_{Au} [30]. From STM observation, formation of a chain has been reported for I on Pt(001) [31].

When observing LEED patterns at LT for the surface adsorbed at LT (figure 8), streaks appear in the (10) direction, which is different from the direction of the streaks observed at RT. This pattern shows that Cl atoms are arrayed along troughs with a periodicity five times as large as the unit cell on the corrugated 5 × 20 surface, i.e. the substrate surface remains reconstructed at LT after Cl adsorption.

The superlattice patterns shown in figures 6 and 7 might be caused by displacement of the topmost Au atoms rather than by Cl atoms. The superspots in figures 6 and 7 are intensive, while the fractional spots observed in the K monolayer on Au(001) are faint [19]. Even if Au atoms should be displaced, the discussion in this paper is not essentially affected. The models in figures 6 and 7 can be imagined as Au displaced structures by replacing shaded circles with open ones. However, the absolute coverage discussed in the next section might be affected, and also the arrangement of adsorbed Cl cannot be determined.

Although the intensity of superspots is strong, we do not consider that Au is necessarily displaced from the lattice point. As shown in figure 5, the intensity of the (10) spot decreases at first and is constant at higher coverage. We consider this to be caused by competition between a decrease of scattered electrons from Au caused by the growing of the Cl overlayer and the ordering process to c(2 × 2). This seems to indicate that it is the top layer that predominantly contributes to the LEED pattern. Therefore, we assume that superlattices are formed by adsorbed Cl, the relation of the temperatures of de-reconstruction (~200 K), phase transition (~150 K), and freezing point of chlorine (~113 K), suggesting that Au atoms are not displaced at LT.

4.2. Origin of the de-reconstruction

First, we discuss the coverage of Cl on Au(001). It is important to estimate the absolute coverage when comparing the de-reconstruction for K and Cl adsorption. As discussed in section 3.1, the integrated intensity of the Cl TDS is proportional to the relative coverage, θ_r. Since the LEED pattern gives the c(2 × 2) structure at the saturation coverage, the absolute coverage of Cl on Au(001) at saturation, θ_a^{sat}, should be either 0.5 or 1. In the case of $\theta_a^{sat} = 1$, a reasonable model for the Cl adsorbate structure can be constructed at LT, as discussed above. The case of $\theta_a^{sat} = 0.5$, on the other hand, is difficult to reconcile with the experimental result of the extinction relation in LEED. Therefore, we conclude that the relative coverage is equal to the absolute coverage, $\theta_r = \theta_a$.

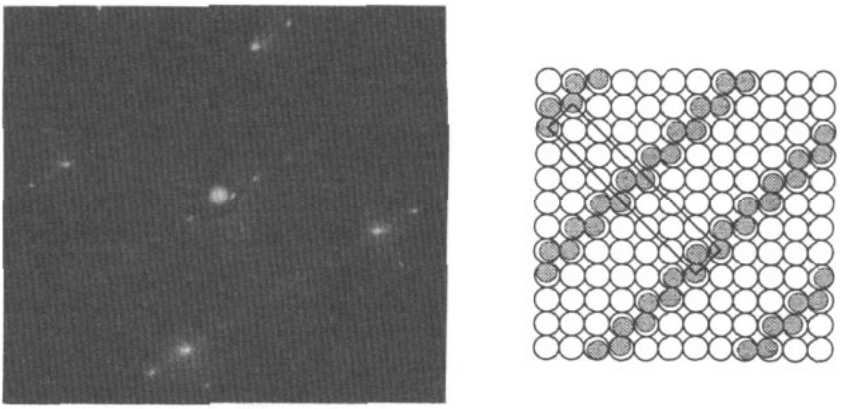

Figure 7. LEED pattern of Cl on Au(001) at LT. Chlorine is adsorbed at $\theta_r > 0.4$ at LT and the surface is annealed at ~800 K. The unit cell is $(6\sqrt{2} \times \sqrt{2})$R45° ($\theta_r \sim 0.34$). $E_p = 60$ eV. The right-hand side shows the structure model (see figure 6). The relative coverage is determined from TDS.

The critical absolute coverage for the de-reconstruction in Cl on Au(001), ~0.06, is similar to that in K on Au(001), ~0.08 [19]. This fact seems to imply that de-reconstruction in Cl adsorption on Au(001) has the same origin as that in K adsorption. We already considered that the driving force of the de-reconstruction in K adsorption on Au(001) is the chemisorption energy of an adsorbate with the surface rather than charge donation from an adsorbate to the substrate [19]. This conclusion is confirmed by the de-reconstruction in Cl adsorption on Au(001), because the direction of the charge transfer between a Cl atom and the substrate is opposite to that in the K case. Furthermore, the absolute value of the charge donation estimated from the coverage dependence of the workfunction change is quite different between Cl and K adsorption, as shown below. In spite of these facts, the de-reconstruction induced by K and Cl adsorption occurs at almost the same coverage.

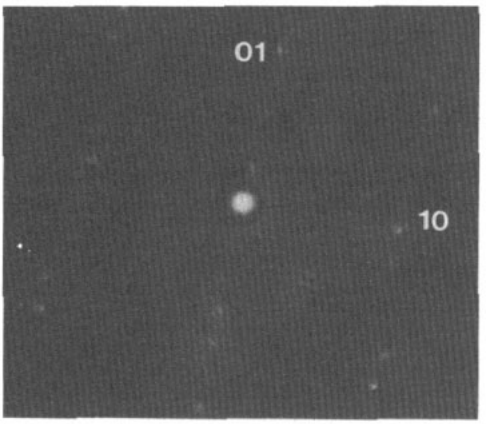

Figure 8. LEED pattern of Cl on Au(001) at LT, when chlorine is adsorbed at LT ($\theta_r \sim 0.6$). $E_p = 60$ eV.

Figure 9 shows the workfunction change ($\Delta\phi$) as a function of coverage for Cl adsorption on the Au(001) surface at RT. The workfunction increases linearly as the coverage

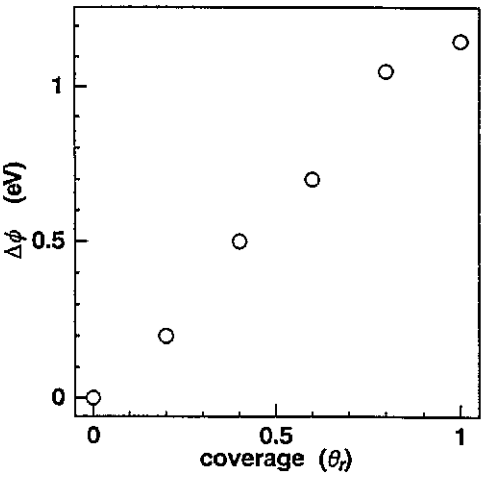

Figure 9. Workfunction change of Cl on Au(001) as a function of Cl coverage at RT.

increases until $\theta_r \sim 0.8$ and $\Delta\phi$ reaches $+1.2$ eV at the saturation coverage. This result is similar to Br on Au(001) [21] and Cl on Au(111) [26]. The linear increase of $\Delta\phi$ can be explained by a scheme that the charge transfer occurs from the substrate (Au) to the adsorbate (Cl), and that the depolarization effect can be ignored in contrast to alkali metal adsorption. In the case of K adsorption on Au(001), the workfunction decreases rapidly at low coverage, and is nearly constant at an absolute coverage of ~0.17 [19]. The absolute value of the gradient in the workfunction change against coverage curve at low coverages in K on Au(001) [19] is much larger than that in the present case of Cl on Au(001). From this result, we consider that the bonding nature between Cl and Au(001) is covalent rather than charge transfer.

As seen in figure 5, the intensity of the (10) and (1/5 0) spots changes gradually until $\theta_r \sim 0.3$ after the critical change at $\theta_r \sim 0.06$. This result shows that the de-reconstruction occurs partially at $\theta_r \sim 0.06$ and is completed at $\theta_r \sim 0.3$. The coverage of ~0.3 coincides with the lowest coverage where long-range ordering of the one-dimensional chains is formed. We consider that the interchain interaction is less effective at $\theta_r < 0.3$, and that the one-dimensional chains interact strongly on the completely de-reconstructed surface at $\theta_r > 0.3$.

It is noted that the intensity of the (10) spot in figure 5 decreases at $0.3 \leqslant \theta_r \leqslant 0.5$, and has a constant value at higher coverage. It is considered that the decrease of intensity is caused by scattering due to a disordered top-layer. At $\theta_r \geqslant 0.5$, this decrease could then be compensated by formation of the ordered c(2 × 2) phase on the top-layer, the intensity of the (10) spot being constant at higher coverage.

4.3. Frustrated desorption of Cl atoms

Both the atomic Cl and molecular Cl_2 species are thermally desorbed from Cl-adsorbed Au(001). In TDS of the Cl species, two peaks appear; one is a broad peak and the other is a prominent sharp peak, as shown in figure 1(*a*). The former peak is due to cracking of a fraction of desorbed Cl_2 and the latter is due to atomic desorption. The desorption energy fitted to this broad peak is ~2 eV, which is a reasonable value for the desorption energy. On the other hand, the apparent desorption energy fitted to the latter peak is higher than 4 eV, which is too high for the desorption energy of adsorbates from the Au surface. Furthermore, the peak position of the latter peak does not change with coverage. Thus, we consider this sharp peak to correspond to explosive desorption. Another prominent feature

in TDS is the constant ratio of the total amount of the desorbed Cl_2 species and that of the desorbed Cl species irrespective of the initial coverage. The atomic Cl is desorbed after Cl_2 has finished, i.e. the critical coverage for the explosive desorption is proportional to the initial coverage. We discuss the physical meaning of these features below.

In general, a sharp TDS peak appears when desorption is accompanied by restructuring of the substrate surface or by transition from a metastable phase to a stable phase. After a constant ratio of Cl atoms is desorbed as Cl_2 species it is supposed that the Cl overlayer is frustrated, resulting in explosive desorption of atomic Cl. If the adsorbate layer is assumed to have a one-dimensional character, this linear relation can be readily interpreted. After the one-dimensional adsorbate chain becomes shorter than a critical length, frustration occurs on the adsorbate layer and/or the substrate surface. The critical length is considered to be independent of the chain density.

The one-dimensional character is consistent with the one-dimensional chain structure for the superlattice shown in figures 6 and 7. At LT, the zigzag chain consists of Cl dimers. This dimerized chain structure suggests Peierls instability. Then, at a high temperature at which thermal desorption occurs, Cl atoms may assemble into a simple monatomic chain structure and valence electrons may be delocalized. A theoretical study shows that the Cl $3p_{\parallel}$ band (parallel component to the surface) forms a metallic phase at high coverages [28]. Thus, it is probable that the Cl chain is frustrated at a critical coverage. Two different origins of the frustrated desorption can be considered. The first one is the instability of a linear chain at low atomic density in the chain. At high atomic density, the chain is stabilized by electron delocalization, while the repulsive potential between adjacent Cl atoms becomes dominant due to electrostatic repulsion at low atomic density in a chain. A critical coverage for the explosive desorption corresponds to the time when the repulsive potential surpasses the chain stabilization energy. Another one is reconstruction of the substrate surface. The adsorbed Cl atoms may be destabilized by the structural change from 1×1 to 5×20. The 1×1 pattern remains until an annealing temperature of 800 K, the 5×20 pattern appearing after annealing above 820 K. The onset of the sharp prominent peak in the TDS is ~800 K. Hence, this sharp peak seems to be caused by frustrated desorption coupled with the reconstruction of the substrate surface.

5. Summary

De-reconstruction was observed when Cl is adsorbed on Au(001) at RT at almost the same absolute coverage as that for K adsorption on Au(001). It is thus considered to be caused by the bonding effect between the adsorbate and the substrate rather than by charge transfer. Various superlattices were observed by LEED, when the sample was cooled down from RT (or higher than RT) to LT (~100 K). The $c(2 \times 2)$ structure was observed at saturation coverage. If these superlattices are due to adsorbed Cl, it is considered that adsorbed Cl atoms form one-dimensional chains, and a repulsive interaction works between adjacent chains. The comparison between TDS of Cl and Cl_2 species gives us a model of the frustrated desorption from the one-dimensional adsorbate chains.

Acknowledgment

The authors thank Gero Herrmann for valuable discussions.

References

[1] Palmberg P W and Rhodin T N 1967 *Phys. Rev.* **161** 161
[2] Van Hove M A, Koestner R J, Stair P C, Biberian J P, Kesmodel L L, Bartos I and Somorjai G A 1981 *Surf. Sci.* **103** 189
[3] Hasegawa T, Kobayashi K, Ikarashi N, Takayanagi K and Yagi K 1986 *Japan J. Appl. Phys.* **25** L366
[4] Magnussen O M, Hotlos J, Behm R J, Batina N and Kolb D M 1993 *Surf. Sci.* **296** 310
[5] Gao X, Edens G J, Hamelin A and Weaver M J 1993 *Surf. Sci.* **296** 333
[6] Wendelken J F and Zehner D M 1978 *Surf. Sci.* **71** 178
[7] Barth J V, Brune H, Ertl G and Behm R J 1990 *Phys. Rev.* B **43** 9307
[8] Samson Y, Rousset S, Gauthier S, Girard J C and Klein J 1994 *Surf. Sci.* **315** L969
[9] Heine V and Marks L D 1986 *Surf. Sci.* **165** 65
[10] Heimann P, Hermanson J, Miosga H and Neddermeyer H 1979 *Phys. Rev. Lett.* **43** 1757
[11] Wu S C, Li H, Quinn J, Tian D, Li Y S, Begley A M, Kim S K, Jona F and Marcus P M 1994 *Phys. Rev.* B **49** 8353
[12] Ercolessi F, Parrinello M and Tosatti E 1986 *Surf. Sci.* **177** 314
[13] Takeuchi N, Chan C T and Ho K M 1991 *Phys. Rev.* B **43** 14363
[14] Fiorentini V, Methfessel M and Scheffler M 1993 *Phys. Rev. Lett.* **71** 1051
[15] Gerlach R L and Rhodin T N 1969 *Surf. Sci.* **17** 32
[16] Behm R J, Flynn D K, Jamison K D, Ertl G and Thiel P A 1987 *Phys. Rev.* B **36** 9267
[17] Häberle P, Fenter P and Gustafsson T 1989 *Phys. Rev.* B **39** 5810
[18] Okada M, Tochihara H and Murata Y 1991 *Phys. Rev.* B **43** 1411
[19] Okada M, Iwai H, Klauser R and Murata Y 1992 *J. Phys.: Condens. Matter* **4** L593
[20] Christensen O B and Jacobsen K W 1992 *Phys. Rev.* B **45** 6893
[21] Bertel E and Netzer F P 1980 *Surf. Sci.* **97** 409
[22] Neumann A, Christmann K and Solomun T 1993 *Surf. Sci.* **287/288** 593
[23] Spencer N D, Goddard P J, Davies P W, Kitson M and Lambert R M 1983 *J. Vac. Sci. Technol.* A **1** 1554
[24] Redhead P A 1962 *Vacuum* **12** 203
[25] Spencer N D and Lambert R M 1981 *Surf. Sci.* **107** 237
[26] Kastanas G N and Koel B E 1993 *Appl. Surf. Sci.* **64** 235
[27] The integrated intensity of a Cl TDS is given by $\theta_r = S^H_{Cl} + S^L_{Cl}$, where S^H_{Cl} and S^L_{Cl} are the integrated intensities of the high-temperature and low-temperature peaks, respectively. Since $\theta_r \propto S_{Cl_2}$ from figure 2, where S_{Cl_2} is the integrated intensity of the Cl_2 TDS, and $S^L_{Cl} \propto S_{Cl_2}$, relations of $S^L_{Cl} \propto \theta_r$ and $S^H_{Cl} \propto \theta_r$ are obtained. The true relative coverage $\theta^t_r = aS^H_{Cl} + bS_{Cl_2}$, where a and b are the detection efficiency of Cl and Cl_2, respectively, is proportional to S^H_{Cl}. Therefore it is concluded that θ^t_r is proportional to θ_r.
[28] Ishida H 1990 *Phys. Rev.* B **41** 12288
[29] Donohue J 1974 *The Structures of the Elements* (New York: Wiley) p 396
[30] Pauling L 1960 *The Nature of the Chemical Bond* 3rd edn (Ithaca, NY: Cornell University Press)
[31] Vogel R and Baltruschat H 1991 *Surf. Sci.* **259** L739